

Hadron-nucleus scattering in the local reggeon model with pomeron loops for realistic nuclei

M.A.Braun, A.Tarasov
S.Peterburg State University, Russia

November 13, 2018

Abstract

Contribution of simplest loops for hadron-nucleus scattering cross-sections is studied in the Local Reggeon Field Theory with a supercritical pomeron. It is shown that inside the nucleus the supercritical pomeron transforms into a subcritical one, so that perturbative treatment becomes possible. The pomeron intercept becomes complex, which leads to oscillations in the cross-sections.

1 Introduction

High-energy hadron-nucleus scattering has long been studied in the framework of the local Regge-Gribov theory with a self-interacting supercritical pomeron. The first successful description of the total cross-section in this approach was presented by A.Schwimmer in 1975 [1] who performed summation of fan diagrams in the limit when the pomeron slope α' was zero. With the advent of the QCD attention has been shifted to self-interacting non-local BFKL pomerons. In this approach an analog of the Schwimmer model has been constructed in the form of the Balitsky-Kovchegov evolution equation [2, 3, 4]. However QCD can reliably describe only the hard region of the dynamics. Soft processes, contributing to the bulk of the total cross-section, are better described by the old-fashioned local reggeon theory, so that the latter remains a useful tool in spite of its venerable age.

Both the old local and new non-local pomeron models have been fully considered and applied only in the quasi-classical tree approximation. Loops have been neglected in both formalisms. This approximation can be justified if the parameter $\gamma = \lambda \exp \Delta y$ is small, with y the rapidity and Δ and λ the pomeron intercept and triple pomeron coupling. Then for a large nuclear target, such that $A^{1/3}\gamma \sim 1$, the tree diagrams indeed give the dominant contribution and loops may be dropped. However with the growth of y the loop contribution becomes not small and this approximation breaks down.

Full calculation of the loop contribution seems to be a formidable task for the non-local QCD pomeron. So it seems to be worthwhile to start with the Local Reggeon Field Theory (LRFT) with a supercritical pomeron. Such a study, apart from its possible lessons for the modern QCD approach, also has an independent value, since, as mentioned, the old LRFT with phenomenological parameters describes the soft dynamics of high-energy strong interactions not so badly. Much work has been done on the influence of loop diagrams in the zero-dimensional LRFT, both theoretically old ago in [5, 6, 7, 8] and numerically recently in [9]. This influence turns out to be decisive for the asymptotic behaviour at large energies and transforms the supercritical pomeron into a weakly

subcritical one with the effective intercept $\propto -\exp(1/\lambda^2)$ where λ is the triple-pomeron coupling assumed to be small.

Unfortunately generalization of these beautiful results to the realistic case of two transverse dimensions is prohibitively difficult. To start with, one is forced to introduce a non-zero value of the slope: otherwise the loop contribution is divergent in the impact parameter. However even in the tree approximation solution of the model with $\alpha' \neq 0$ is only possible numerically. Second, the model in $d_T = 2$ needs renormalization in the ultraviolet. And, most important, the method used to solve the model in $d_T = 0$, which is to study the corresponding quantum-mechanical system and the relevant Schrödinger equation, is inapplicable in the realistic case, since instead of ordinary differential equations one arrives at equations with functional derivatives. In fact summation of all loop contributions is equivalent to a complete solution of the corresponding quantum field theory, the task which seems to be beyond our present possibilities. So at most one can hope to obtain some partial results which might shed light onto the properties of the model with loops. There were several attempts to study the high-energy behaviour of the LRFT with a supercritical pomeron using different approximate techniques and giving contradicting results [10], [11].

In our previous study, instead of trying to solve the model for the purely hadronic scattering we considered the hadron-nucleus scattering and propagation of the pomeron inside the heavy nucleus target [12]. Moreover to avoid using numerical solution of the tree diagrams contribution with diffusion in the impact parameter, we concentrated on the case of a constant nuclear density which allowed to start with the known analytical solutions. We have found that the nuclear surrounding transforms the pomeron from the supercritical one with intercept $\epsilon > 0$ to a subcritical one with the intercept $-\epsilon$. Then Regge cuts, corresponding to loop diagrams, start at branch points located to the left of the pomeron pole and their contribution is subdominant at high energies. As a result the theory acquired the properties similar to the standard LRFT with a subcritical pomeron and allows for application of the perturbation theory.

However the adopted approximation of a constant nuclear density in the whole space was obviously too crude. In fact it did not allow to make convincing conclusions about the physical cross-sections, so that we had to recur to some weakly supported guesses on this point. In this paper we try to improve our treatment and consider realistic nuclear targets which occupy finite space volume. This enables us to predict the influence of loops on the total cross-section and study applicability of the perturbative approach to hadron-nucleus scattering with pomeron loops.

Our results depend on the behaviour of the nuclear profile function $T(b)$ at large values of the impact parameter b . For a finite nucleus with $T(b) = 0$ at $b > R_A$ all our conclusions found in [12] for constant $T(b)$ remain valid and one can apply perturbative methods to study the loop contribution. However for an infinite nucleus, for which $T(b)$ exponentially falls with b but never vanishes at finite b , the loop influence is perturbative only inside the nucleus, at not too large b . At very large b , well outside the bulk of the nuclear matter, the loop contribution blows up and the cross-section becomes unperturbative.

The paper is organized as follows. In the next section we introduce the model and reformulate it to describe the loops in the nuclear surrounding. In Section 3 we introduce a quasi-local approximation to constructively treat the case of realistic nuclei. In Section 4 we formulate the appropriate Dyson equation for the amplitude with loops. Our numerical results for total pPb and pCu cross-sections are presented in Section 5. Finally Section 6 draws some conclusions.

2 Local pomeron in the nuclear field

The LRFT model is based on two pomeron fields $\phi(y, b)$ and $\phi^\dagger(y, b)$ depending on the rapidity y and impact parameter b , with a Lagrangian density

$$L = L_0 + \lambda\phi^\dagger\phi(\phi + \phi^\dagger) + g\rho\phi. \quad (1)$$

Here the free Lagrangian density is

$$L_0 = \phi^\dagger\left(\frac{1}{2}\overset{\leftrightarrow}{\partial}_y - \alpha'\nabla_b^2 + \epsilon\right)\phi \equiv \phi^\dagger S\phi \quad (2)$$

where ϵ is the intercept minus unity and α' is the slope. The source term describing interaction with the nuclear target at low energies is

$$g\rho(y, b) = gAT(b)\delta(y). \quad (3)$$

where g is the pomeron-nucleon coupling constant and $T(b)$ the profile function of the nucleus. For a supercritical pomeron $\epsilon > 0$ and $\lambda < 0$.

The classical equation of motion are

$$\frac{\delta L}{\delta\phi} = -\partial_y\phi^\dagger - \alpha'\nabla_b^2\phi^\dagger + \epsilon\phi^\dagger + \lambda\phi^{\dagger 2} + 2\lambda\phi\phi^\dagger + g\rho = 0 \quad (4)$$

and

$$\frac{\delta L}{\delta\phi^\dagger} = \partial_y\phi^\dagger - \alpha'\nabla_b^2\phi + \epsilon\phi + \lambda\phi^2 + 2\lambda\phi^\dagger\phi = 0. \quad (5)$$

From the latter equation we find $\phi = 0$ and the equation for ϕ^\dagger takes the form

$$\partial_y\phi^\dagger = -\alpha'\nabla_b^2\phi^\dagger + \epsilon\phi^\dagger + \lambda\phi^{\dagger 2}, \quad (6)$$

with an initial condition

$$\phi^\dagger(y = 0) = g\rho \quad (7)$$

Equation (6) describes evolution of the pomeron field in rapidity and its diffusion in the impact parameter inside the nucleus. We denote the solution of the classical equation of motion (6) with the initial condition (7) as $\xi(y, b)$

To go beyond the classical approximation and thus study loops we make a shift in the quantum field ϕ^\dagger :

$$\phi^\dagger(y, b) = \phi_1^\dagger(y, b) + \xi(y, b) \quad (8)$$

and reinterpret our theory in terms of fields ϕ and ϕ_1^\dagger . In the Lagrangian terms linear in ϕ vanish due to the equation of motion for ξ and we obtain

$$L = \phi_1^\dagger(S + 2\lambda\xi)\phi + \lambda\xi\phi^2 + \lambda\phi_1^\dagger\phi(\phi_1^\dagger + \phi). \quad (9)$$

This Lagrangian corresponds to a theory in the vacuum with the pomeron propagator in the external field $f(b, y) = 2\lambda\xi(y, b)$

$$P = -(S + 2\lambda\xi)^{-1}, \quad (10)$$

the standard triple interaction and extra interaction described by the term $\lambda\xi\phi^2$. This new interaction corresponds to transition of a pair of pomerons into the vacuum at point (y, b) with a vertex $\lambda\xi(y, b)$, see Fig. 1.

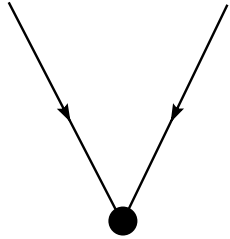


Figure 1: The new vertex for two-pomeron annihilation, which appears after the shift in field ϕ^\dagger

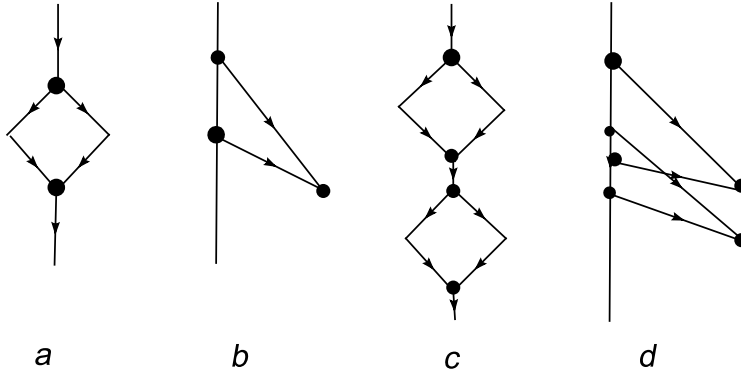


Figure 2: Some simple loop diagrams for the pomeron Green function

Loops can be formed both by the standard interaction and the new one. In the latter case they are to be accompanied by at least a pair of standard interactions. Diagrams with a few simple loops in the Green function are illustrated in Fig. 2. One immediately observes that a loop formed by the standard interaction has the order λ^2/α' and requires renormalization. A loop formed by the new interaction has the order λ^3/α' and is finite.

The amplitude is obtained as a tadpole $g < \phi_1^\dagger(y, b) >$. The simplest diagrams for it contain one loop and are shown in Fig. 3 a, b. Diagrams with more loops are shown in Figs. 3 c, d.

Propagator (10) in the external field $f(y, b) = 2\lambda\xi(y, b)$ where $\xi(y, b)$ is the classical field ϕ^\dagger satisfies the equation

$$\frac{\partial P(y, b|y', b')}{\partial y} = (\epsilon - \alpha' \nabla_b^2) P(y, b|y', b') + f(y, b) P(y, b|y', b') \quad (11)$$

with the boundary conditions

$$P(y, b|y', b') = 0, \quad y - y' < 0, \quad P(y', b|y', b') = \delta^2(b - b'). \quad (12)$$

In the general case propagator P can only be calculated numerically, just as the external field $f(y, b)$. Its analytic form can be found in two cases [12].

If the slope $\alpha' = 0$ then one finds

$$f(y, b) = -\frac{\epsilon a(b) e^{\epsilon y}}{p(y, b)} \quad (13)$$

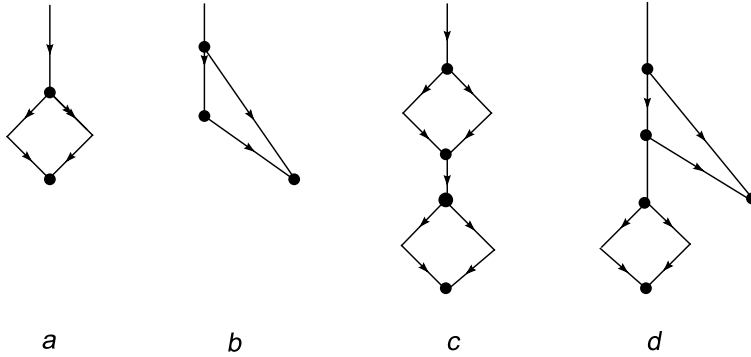


Figure 3: Diagrams with one loop (*a*, *b*) and two loops (*c* and *d*) for the scattering amplitude

and

$$P(y, b|y', b') = \delta^2(b - b')P_0(y, y', b), \quad P_0(y, y', b) = e^{\epsilon(y-y')} \frac{p^2(y', b)}{p^2(y, b)}, \quad (14)$$

where

$$a(b) = -\frac{\lambda g \rho(b)}{\epsilon} > 0 \quad (15)$$

and

$$p(y, b) = 1 + a(b)(e^{\epsilon y} - 1). \quad (16)$$

Propagator $P_0(y, y', b)$ corresponds to the zero-dimensional theory with $a(b)$ as an external parameter. It is remarkable that at large y propagator $P_0(y, y', b) \simeq \exp(-\epsilon y)$, that is behaves as the free propagator with the opposite sign of ϵ and so vanishes at $y \rightarrow \infty$. In contrast to the free propagator it corresponds to a subcritical pomeron.

The second case which admits an analytic solution for the propagator is that of the nuclear matter, that is the case when the profile function is constant in all the transverse space

$$T(b) = T_0. \quad (17)$$

Then the classical field ξ and the external field $f = 2\lambda\xi$ become b -independent and the propagator in this field takes the form

$$P(y, b|y', b') = \frac{1}{4\pi\alpha'(y - y')} e^{\epsilon(y-y') - \frac{(b-b')^2}{4\alpha'(y-y')}} \frac{p^2(y')}{p^2(y)}. \quad (18)$$

where $p(y)$ is given by (16) with a constant a . Note an especially simple case when $a = 1$ and $p(y) = \exp \epsilon y$. Then the propagator in the external field coincides with the free propagator with the opposite sign of ϵ , so that the theory formally corresponds to a subcritical pomeron model with an additional interaction shown in Fig. 1

3 Realistic nucleus

The full treatment of the scattering on a realistic nucleus with the profile function $T(b)$ which varies with b and vanishes as $b \rightarrow \infty$ requires solution of the equations (6) for the pomeron field and (11) for the propagator in the found external field $f(y, b)$. Both tasks can be done only numerically and look hardly feasible.

To facilitate the problem we shall use the approximation of a weakly varying $T(b)$. Equivalently we assume that the slope α' , which governs diffusion in the impact parameter, is small. Accordingly we shall put α' to zero wherever possible. In particular we shall use expression (13) for the field at fixed value b of the impact parameter. For the propagator we shall use expression (14) so long as it stands alone. However we cannot do this in pomeron loops, where it is squared leading to a divergence at $\alpha' \rightarrow 0$.

For loops we shall restrict ourselves with the leading term as $\alpha' \rightarrow 0$ and so use the leading approximation for the propagator inside the loop in this limit but not the limit itself. This leading approximation obviously coincides with the approximation of a slowly varying nuclear field and is given by Eq. (18) with p depending on b in accordance with definition (16). One can see it from the following reasoning. Let us seek the propagator satisfying Eq. (11) as a product

$$P(y, b|y', b') = P_0(y, y', b)P_1(y, b|y', b') \quad (19)$$

with the known $P_0(y, y', b)$ defined in Eq. (14). Then we find an equation for P_1

$$P_0(y, y', b) \frac{dP_1(y, b|y', b')}{dy} = \alpha' \nabla_b^2 P_0(y, y', b) P_1(y, b|y', b).$$

Assuming the smallness of α' and non-singularity of P_0 as a function of b or equivalently a weak dependence of P_0 on b we can neglect action of the derivatives in b on $P_0(y, y', b)$ to obtain an equation for P_1

$$\frac{\partial P_1(y, b|y', b')}{\partial y} = \alpha' \nabla_b^2 P_1(y, b|y', b).$$

Solution of this equation brings us to propagator (18).

With this approximation we now calculate the simplest loops which appear in the theory paying special attention to their b -dependence.

The simple loop Fig. 2a is given by the expression

$$\Sigma_1(y, b|y', b') = -2\lambda^2 P^2(y, b|y', b') + \Delta\epsilon\delta^2(b - b')\delta(y - y'). \quad (20)$$

The second term comes from the intercept renormalization. Using (18) we find

$$\Sigma_1(y, b|y', b') = -2\lambda^2 \frac{p^4(y', b)}{p^4(y, b)} \left(\frac{1}{4\pi\alpha'(y - y')} \right)^2 e^{2\epsilon(y - y') - \frac{(b - b')^2}{2\alpha'(y - y')}} + \Delta\epsilon\delta^2(b - b')\delta(y - y'). \quad (21)$$

The exponential factor depending on $(b - b')^2$ obviously becomes proportional to $\delta^2(b - b')$ in the limit $\alpha' \rightarrow 0$

$$\frac{1}{2\pi\alpha'(y)} e^{-\frac{b^2}{2\alpha'y}} \underset{\alpha' \rightarrow 0}{\rightarrow} \delta^2(b). \quad (22)$$

Thus we obtain at small α'

$$\Sigma_1(y, b|y', b') = -\delta^2(b - b') \frac{\lambda^2}{4\pi\alpha'(y - y')} e^{2\epsilon(y - y')} \frac{p^4(y', b)}{p^4(y, b)} + \Delta\epsilon\delta^2(b - b')\delta(y - y'). \quad (23)$$

Note that at fixed b and rapidities Σ_1 is finite. Ultraviolet divergence appears in the process of integration over rapidity at $y - y' = 0$. Regularizing this integration by cutting it at $y - y' = y_{min}$ one can express

$$\Delta\epsilon = -\frac{\lambda^2}{4\pi\alpha'} \ln(c_R y_{min}) \quad (24)$$

with c_R a renormalization constant taking place of $\Delta\epsilon$.

Now we pass to the simplest new self-mass of Fig. 2b. It does not need renormalization and is given by

$$\Sigma_2(y, b|y', b') = 4\lambda^3 P(y, b|y' b') \int dz d^2 c \xi(z, c) P(y, b|z, c) P(y', b'|z, c). \quad (25)$$

With the approximate form (18) for the propagator we find a product of exponential factors depending on impact parameters

$$\frac{1}{(4\pi\alpha')^3 (y - y')(y - z)(y' - z)} e^{-\frac{(b-b')^2}{4\alpha'(y-y')} - \frac{(b-c)^2}{4\alpha'(y-z)} - \frac{(b'-c)^2}{4\alpha'(y'-z)}}$$

to be integrated over z and c . Integration over c converts this into

$$\frac{1}{(4\pi\alpha')^2 (y - y')(y + y' - 2z)} e^{-\frac{(b-b')^2}{4\alpha'(y-y')} - \frac{(b-b')^2}{4\alpha'(y+y'-2z)}} \rightarrow \frac{1}{8\pi\alpha'} \delta^2(b - b') \text{ at } \alpha' \rightarrow 0.$$

So in our approximation we find the new self-mass

$$\Sigma_2(y, b|y', b') = -\delta^2(b - b') \theta(y - y') \frac{4\lambda^2 \epsilon a(b)}{8\pi\alpha'} \int_0^y \frac{dz}{y - z} e^{\epsilon(2y-z)} \frac{p^3(z, b)}{p^4(y, b)}. \quad (26)$$

4 Amplitude at fixed impact parameter

In the adopted approximation all integrations over intermediate impact parameters are performed with the help of δ functions and at fixed impact parameter b the final amplitude $T(y, b)$ is a function of b presented as a multiple integral over intermediate rapidities. So the whole picture is local in b .

The propagator (14) in the external field has the crucial property that it decreases with y as $y \rightarrow \infty$:

$$P(y, y', b)_{(y-y') \rightarrow \infty} \rightarrow e^{-\epsilon(y-y')} f(y', b). \quad (27)$$

Because of this property internal integrations over rapidities do not lead to contributions which grow faster than the lowest order term. This ensures convergence of the perturbative expansion at small enough values of λ

Introduction of loops into the amplitude \mathcal{A} is achieved by the Dyson equation

$$\mathcal{A}(y, b) = \mathcal{A}^{(0)}(y, b) + \int_0^y dy_1 \int_0^{y_1} dy_2 P(y, y_1, b) \Sigma(y_1, y_2, b) \mathcal{A}(y_2, b), \quad (28)$$

where the lowest order term is

$$\mathcal{A}^{(0)}(y, b) = -\frac{a(b) e^{\epsilon y}}{\lambda p(y, b)} \quad (29)$$

with $p(y, b)$ given by (16) and the pomeron self mass $\Sigma(y, b|y' b')$ presented in our approximation as

$$\Sigma(y, b|y', b') = \delta^2(b - b') \Sigma(y, y', b) \quad (30)$$

In accordance with the convergence of the perturbative expansion, in the first approximation we take

$$\Sigma(y, b|y', b') = \Sigma_1(y, b|y', b') + \Sigma_2(y, b|y', b') \quad (31)$$

where Σ_1 and Σ_2 are the 2nd and 3d order self-mass contributions studied above. We present

$$\mathcal{A}(y, b) = \mathcal{A}^{(0)}(y, b) r(y, b). \quad (32)$$

The equation for $r(y)$ takes the form

$$r(y, b) = 1 + X_1(y, b) + X_2(y, b), \quad (33)$$

where X_1 and X_2 are parts coming from Σ_1 and Σ_2 respectively. Explicitly

$$X_1 = -\frac{C}{p(y, b)} \ln(c_R y) \int_0^y dy_1 p(y_1, b) r(y_1) - \frac{C}{p(y, b)} \int_0^y \frac{dz}{z} (\omega(y, z, b) - \omega(y, 0, b)), \quad (34)$$

where

$$C = \frac{\lambda^2}{4\pi\alpha'} \quad (35)$$

and

$$\omega(y, z, b) = e^{\epsilon z} \int_z^y dy_1 \frac{p^3(y_1 - z, b)}{p^2(y_1, b)} r(y_1 - z, b). \quad (36)$$

The part $X_2(y)$ is

$$X_2(y) = -\frac{2a(b)\epsilon C}{p(y, b)} \int_0^y dy_1 \frac{e^{\epsilon y_1}}{p^2(y_1, b)} \int_0^{y_1} \frac{dy_3}{y_1 - y_3} p^3(y_3, b) e^{-\epsilon y_3} \int_{y_3}^{y_1} dy_2 \frac{e^{\epsilon y_2}}{p(y_2, b)} r(y_2, b). \quad (37)$$

Eq. (33) contains the renormalization constant c_R as a parameter. To fix it we use the prescription proposed in [12]. The contribution to $\mathcal{A}(y, b)$ of a single loop is

$$\mathcal{A}^{(1)}(y, b) = \mathcal{A}^{(0)}(y, b) r^{(1)}(y, b) \quad (38)$$

where

$$r^{(1)}(y, b) = (X_1(y, b) + X_2(y, b))_{r(y, b)=1}. \quad (39)$$

The right-hand side of Eq. (39) can be calculated and shown to have a finite limit at $y \rightarrow \infty$

$$r^{(1)}(y, b)_{y \rightarrow \infty} = -\frac{\lambda^2}{4\pi\alpha'\epsilon} \left(\ln \frac{c_R}{2\epsilon} + 1 - C_E \right), \quad (40)$$

where C_E is the Euler constant. Remarkably this limit does not depend on b and is universal. So one can use it to fix the renormalization constant by requirement that this limit is zero:

$$c_R = 2\epsilon e^{C_E - 1}. \quad (41)$$

This means that at large rapidities the loop contribution vanishes, so that one defines the pomeron intercept from the asymptotic of the amplitude requiring it to coincide with the lowest order term.

With all this, one should be careful in applying these results for different values of impact parameter b . The decrease of the propagator $P(y, y', b)$ obviously starts when $p(y, b)$ begins to rise, which requires $a(b)e^{\epsilon y} \gg 1$ or

$$e^{\epsilon y} \gg \frac{1}{a(b)}$$

It follows that for very small $a(b)$ the actual decrease will start at very large rapidities. At $a(b)e^{\epsilon y} \sim 1$ the propagator will have order $1/a(b)$. In other words, at small $a(b)$ we expect the ratio $r(y, b)$ to rise with rapidity from unity to a large value $1/a(b)$ at $\epsilon y = y_0 \sim -\ln(a(b))$ and then

drop to zero at $y \gg y_0$. At its maximum the loop contribution will be greater than the lowest order by factor

$$\zeta = \frac{\lambda^2}{4\pi\alpha'\epsilon a(b)}, \quad (42)$$

where ϵ in the denominator comes from the essential interval of integration over intermediate rapidities. If the triple pomeron coupling constnt λ is small enough this does not prevent using perturbation theory since $\lambda^2/a(b) \sim \lambda$. However it does bring difficulties if one fixes λ and then varies $a(b)$ to very small values at large b . This point is essential in the application of the model to realistic nuclei studied in the next sections.

5 Numerical results

The total hadron-nucleus cross-section is given by twice the imaginary part of the hA amplitude, integrated over all values of the impact parameter. To take into account unitarity at fixed b we glauberize the contribution from a single fan with loops, which implies that the projectile hadron may emit any number of such structures.

$$\sigma(y) = 2 \int d^2b \left(1 - e^{g\mathcal{A}(y,b)} \right). \quad (43)$$

To calculate $\mathcal{A}(y,b)$ we have solved the Dyson equation (28) for proton-lead and proton-copper collisions ($A = 207$ and 64) at each value of b with the pomeron self-mass given by the sum of lowest order loops $\Sigma_1 + \Sigma_2$.

We used more or less standard values for the pomeron parameters extracted from the experimental data on proton-proton scattering

$$\epsilon = 0.08, \quad \alpha' = 0.2 \text{ GeV}^{-2}, \quad \lambda = -0.48 \text{ GeV}^{-1}, \quad g = 5.94 \text{ GeV}^{-1}. \quad (44)$$

Note that ϵ and g can be rather reliably taken directly from the proton-proton inelastic cross sections. The rest of the parameters is not so well established and model dependent. Our set agrees with the parametrization used in [13]. With the set (44) the value of parameter ζ which controls the relative order of loop contribution and so applicability of perturbative treatment is of the order $1/a(b)$. For heavy nuclei the maximal value of $a(b)$ is $a(0) \sim 1$. So strictly speaking for realistic nuclear scattering the used values of λ do not lie within the applicability of perturbative treatment. This circumstance has to be taken into account in analyzing our results with λ given in (44), which should be taken as qualitative.

We considered two models for the spatial structure of the nuclear target. The simplest one assumes the nucleus to be a sphere with a constant nuclear density of radius

$$R_A = A^{1/3} R_0, \quad r_0 = 1.15 \text{ fm}.$$

This is the nuclear model most suitable for our approach, since it excludes the region of very small nuclear densities ouside the nucleus in which the perturbative treatment is impossible due to large values of ζ . In this case the found hA cross-sections are shown in Fig. 4 as a function of rapidity y . To see the influence of loops we also presented the cross-sections without loop contribution, which correspond to the monotonous curves. To clearly see the A -dependence we rescaled the pCu cross-section to be equal to the pPb one at small y . As one observes, the loop contribution is quite noticeable and leads to oscillations in the cross-sections. The origin of oscillations is understandable

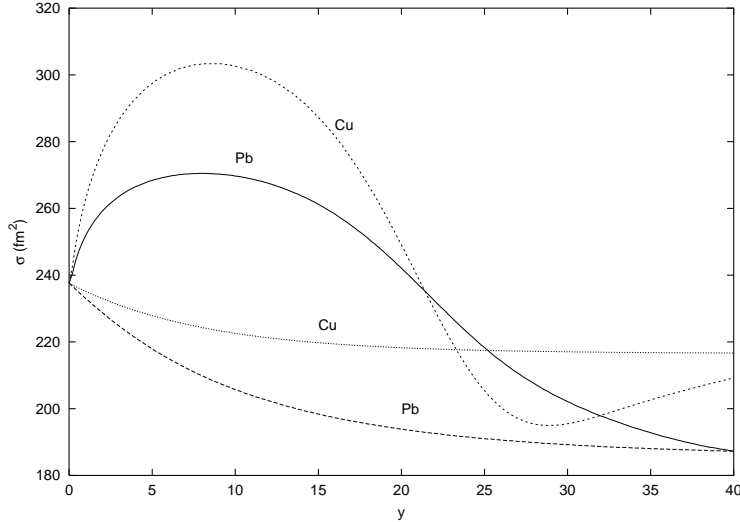


Figure 4: pPb and pCu cross-sections on the target nucleus as a sphere with a constant density. The oscillating (monotonous) curves corresponds to presence (absence) of pomeron loops. The pCu cross-sections are multiplied by 2.55 to coincide with the pPb one at small y

from the fact that with loops the original pomeron pole splits into two complex conjugated poles, which remain on the physical sheet due to the absorptive nature of the loop (negative signs in (23) and (26)). The A dependence is quite strong and also understandable. With the growth of A the damping effect of the nuclear surrounding grows, so that the cross-sections generally become relatively smaller, both with and without loops.

As a second model for the nucleus density we considered the standard Woods-Saxon one. Such a nucleus has no finite dimension and we have to vary b from zero to infinity. With the growth of b outside the nucleus parameter $a(b)$ becomes exponentially small and formal application of our formulas becomes impossible because of the growth of the perturbative parameter ζ . To overcome this difficulty we take into account that at b outside the nucleus the projectile practically interacts with a free nucleon and so its amplitude is wholly determined by the single pomeron exchange without any loop insertions, which are assumed to be incorporated into the effective pomeron parameters. So we have introduced a cutoff into the loop contributions multiplying them by

$$c_f = \frac{a(b)}{a_0 + a(b)}$$

and choosing $a_0 = a(R_A + \Delta b)$ with $b = 1.5$ fm. The resulting pPb cross-sections are presented in Fig. 5 again together with the cross-sections without loops, which correspond to the monotonous curve. The found cross-sections show the same qualitative behaviour as with the finite nucleus, although the absolute values and the amplitude of oscillations are somewhat greater. The cross-sections without loops naturally grow faster than for a finite nucleus because of the contribution of the nuclear halo.

The amplitude of oscillations is determined by the value of λ . With smaller λ 's the oscillations die out. To see that we repeated our calculations with a smaller value of the triple pomeron coupling constant found in [14] $\lambda = -0.069$, that is nearly ten times smaller than in (44). With such λ the perturbation parameter drops to $\zeta \sim 1/5$ inside the nucleus, so that perturbative expansion

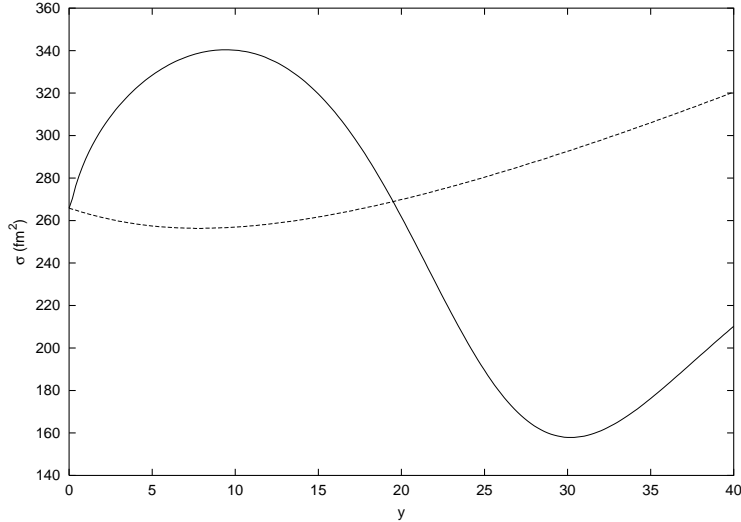


Figure 5: pPb cross-sections on the target nucleus with the Woods-Saxon density. The oscillating (monotonous) curve corresponds to presence (absence) of pomeron loops

becomes reasonable. Our results for pPb cross-sections with $\lambda = -0.069$ are shown in Fig. 6. We observe that the influence of loops is quite small. It grows with rapidity and becomes noticeable at $y \sim 30 \div 40$ only to vanish in the end at still higher rapidities. Comparing with Figs. 4 and 5 one also observes that with smaller λ the cross-sections rise faster with y due to the behaviour of the zero-order term (29). At very small λ the damping exersized by fanning is small and $\mathcal{A}^{(0)}$ grows like the pomeron itself.

6 Conclusions

We studied the contribution of the two simplest loops in the local reggeon field theory with a supercritical pomeron in the nucleus. We applied a quasi-local approximation which assumes that the slope α' is small and can be put to zero in all places except in the loops where the leading term at $\alpha' \rightarrow 0$ has been retained. Our results confirm the conclusion reached in [12] that the nuclear surrounding transforms the supercritical pomeron with the intercept $\alpha(0) - 1 = \epsilon > 0$ into the subcritical one with the intercept $-\epsilon$. As a result, at high energies the pomeron Green function vanishes and contributions from multipomeron exchanges vanish still faster according to the standard predictions for the subcritical pomeron. However this phenomenon becomes effective at different energies depending on the nuclear density. At small densities the Green function begins to decrease at very high rapidities far beyond our present experimental possibilities. And in the intermediate region loop contributions may become large if the triple pomeron coupling constant λ is not small enough.

So while the general conclusion about the validity of the perturbative treatment is true, its practical realization depends on the value of λ and is determined by the perturbative parameter ζ defined in (42). Unfortunately with the standard values (44) for λ parameter $\zeta \sim 1$ and perturbative treatment is dubious. Higher order loops have to be included into the picture to have quantitative results. With smaller values of λ the loop contribution becomes small and perturbation approach is justified.

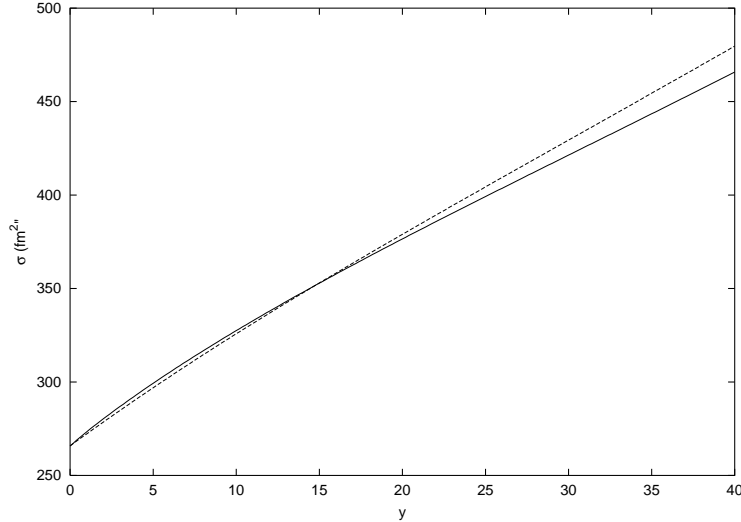


Figure 6: pPb cross-sections on the target nucleus with the Woods-Saxon density and $\lambda = -0.069$. The lower (upper) curve on the right side corresponds to presence (absence) of pomeron loops

The influence of loops shows itself in oscillations in rapidity of the cross-sections. These oscillations are due to the complex character of the pomeron pole once loops are included. Due to the wrong sign of the pomeron self-mass the pomeron poles does not move to the second sheet of the energy plane as with normal particles but stays on the physical sheet acquiring a nonzero imaginary part. Of course with very small λ oscillations are small and have a very long period in y . However with greater λ they are clearly visible, as illustrated in Figs. 4 and 5

On the practical side our results point to yet another possibility to experimentally measure the value of the triple-pomeron coupling constant λ on which the behaviour of the cross-sections with energy critically depends. To exclude the region of impact parameters b well outside the nucleus, where our treatment becomes invalid, one may select events in which the collisions occur inside the nucleus by requiring the multiplicity of produced particles to be large enough.

From the theoretical point of view we consider our results to be promising as a basis for treating loop contributions in the perturbative QCD. It seems to be advantageous to study them in the nuclear surrounding, which makes the perturbative approach at high energies much more tractable.

7 Acknowledgments

This work has been supported by grants RFFI 09-012-01327-a and RFFI-CERN 08-02-91004.

References

- [1] A.Schwimmer, Nucl.Phys, **B 94** (1975) 445.
- [2] I.I.Balitsky, Nucl. Phys. **B 463** (1996) 99.
- [3] Yu.V.Kovchegov, Phys. Rev **D 60** (1999) 034008; **D 61** (2000) 074018.
- [4] M.A.Braun, Eur. Phys. J. **C 16** (2000) 337.

- [5] D.Amati, L.Caneschi and R.Jengo, Nucl. Phys. **101** (1975) 397.
- [6] V.Alessandrini, D.Amati and R.Jengo, Nucl.Phys. **B 108** (1976) 425
- [7] R.Jengo, Nucl. Phys. **B 108** (1976) 425;
- [8] M.Ciafaloni, M.Le Bellac and G.C.Rossi, Nucl. Phys. **B130** (1977) 388.
- [9] M.A.Braun and G.P.Vacca, Eur. phys. J **C 50** (2007) 857.
- [10] H.D.Abarbanel, J.B.Bronzan, A.Schwimmer and R.Sugar, Phys. Rev. **D 14** (1976) 632.
- [11] D.Amati, M.Le Bellac, G.Marchesini and M.Ciafaloni, Nucl. Phys. **B 112** (1976) 107.
- [12] M.A.Braun and A.Tarasov, Eur. Phys. J **C 58** (2008) 383.
- [13] N.Armesto, A.B.Kaidalov, C.A.Salgado and K.Tywoniuk, arXive:1001.3021 [hep-ph].
- [14] E.Gotsman, A.Kormilitzin, E.Levin and U.Maor, arXive:0912.4689 [hep-ph].